Journal of *Marine Science and Engineering*

MDPI

Article

Shifts in the Assemblage of Summer Mesopelagic Fish Larvae in the Gaoping Waters of Southwestern Taiwan: A Comparison between El Niño Events and Regular Years

Hung-Yen Hsieh [1,*], Wen-Tseng Lo [2], Chien-Chun Liao [1] and Pei-Jie Meng [3,4,*]

[1] Graduate Institute of Marine Biology, National Dong Hwa University, Checheng, Pingtung 944401, Taiwan; sandy.0616@gmail.com
[2] Department of Marine Biotechnology and Resources, National Sun Yat-sen University, Kaohsiung 80424, Taiwan; lowen@faculty.nsysu.edu.tw
[3] General Education Center, National Dong Hwa Shoufeng Campus University, Haulien 974301, Taiwan
[4] National Museum of Marine Biology and Aquarium, Pingtung 94450, Taiwan
* Correspondence: hyhsieh@gms.ndhu.edu.tw (H.-Y.H.); pjmeng@gms.ndhu.edu.tw (P.-J.M.)

Abstract: We investigated changes in the assemblages of summer mesopelagic fish larvae between El Niño events and regular years in 2014–2018 and evaluated their relationships with the hydrographic conditions of the Gaoping waters off southwestern Taiwan. Seventy-five taxa or morphotypes were identified, with five types of *Benthosema pterotum* (31.2%), *Diaphus* slender type (19.9%), *Cyclothone alba* (7.2%), *Diaphus* stubby type (5.9%), and *Vinciguerria nimbaria* (4.4%) being most common during the study period. The hydrographic conditions of the Gaoping waters were likely influenced by large-scale climate change via oceanic physical processes. Apparently higher seawater temperature, mixed layer depth, and lower salinity in the upper 100 m were observed at the end of the strong El Niño events (summer 2016). In addition, the certain dominant taxa exhibited contrasting patterns between El Niño events and regular years. In this study, although the abundance and composition of mesopelagic fish larvae assemblage were not influenced directly by changes in large-scale climatic conditions, the occurrence of mesopelagic fish larvae was related to seawater temperature, salinity, and chlorophyll a concentration. We speculated that despite the abundant food availability and the more mesopelagic fish larvae onto the Gaoping waters transported by the increased inflow of the South China Sea Surface Current during El Niño events, the higher temperature and lower salinity at the inshore upper waters might be unsuitable for mesopelagic fish larvae, possibly resulting in low egg and larval survival.

Keywords: terrestrial runoff; larval transport; climate change; southwesterly monsoon; Taiwan Strait

Citation: Hsieh, H.-Y.; Lo, W.-T.; Liao, C.-C.; Meng, P.-J. Shifts in the Assemblage of Summer Mesopelagic Fish Larvae in the Gaoping Waters of Southwestern Taiwan: A Comparison between El Niño Events and Regular Years. *J. Mar. Sci. Eng.* **2021**, *9*, 1065. https://doi.org/10.3390/jmse9101065

Academic Editor: Dariusz Kucharczyk

Received: 1 September 2021
Accepted: 22 September 2021
Published: 28 September 2021

1. Introduction

Mesopelagic fishes, a group of small fishes, are a key component of marine ecosystems. They are numerically dominant in the oceanic fish assemblage of all temperate and tropical waters in the world, with Myctophiformes and Stomiiformes species being the main representatives [1,2]. Although the size of mesopelagic fishes is small, the trawling estimates suggest that the biomass of mesopelagic fishes is at least 10 billion tons [3], which is about 100 times the annual tonnage captured worldwide by fisheries [4]. Larvae of mesopelagic fishes develop in the productive upper 200 m layer [5,6] and then move to the 200–1000 m mesopelagic layer when they begin to transform from the larval to the juvenile stage [7,8]. Therefore, mesopelagic fishes play an essential role in energy pathways through the water column, linking secondary producers to higher level consumers [9,10]. Meanwhile, they constitute an important vector of carbon fluxes in marine ecosystems, being the epipelagic-benthic coupling by the diel vertical migration [11].

Distribution and composition of fish larvae assemblage is complex in tropical and temperate continental shelf waters throughout the world [12–14]. The presence of fish

larvae assemblage in the continental shelf can be associated with the spawning patterns of adult fishes, larval behavior, and oceanographic processes that transport fish larvae from the ocean to the continental shelf [7,15,16]. Consequently, investigations of fish larvae assemblage not only help to elucidate their early life strategies, but also reveal the short-term oceanographic conditions and biological properties of the surveyed area [13,17]. The survival of the early life stages of fishes is pivotal for determining the annual recruitment of fish [18,19]. In recent decades, at which strong changes in climatic conditions usually occur, the environmental fluctuations alter the structure and dynamic of marine ecosystems [20,21]. Notably, climbing temperatures have been suggested to change the physiological functioning [22,23], migratory behavior [24,25], and spawning frequency [26,27] of fishes, leading to shifts in the size structure, spatial distribution, and seasonal occurrence of populations. The sensitivity of the early life stages of fishes to these changes, however, make fish larvae potentially a good sentinel for the regional climate variation and ecosystem shift [28–30].

The Gaoping waters, located on southwestern Taiwan, are part of the tropical western North Pacific Ocean. Two main currents are present on the Gaoping waters: the warm and low-salinity South China Sea Surface Current (SCSSC) and the warm and highly saline Kuroshio Branch Current (KBC) [31,32]. During the dry season (November to April), the prevailing northeasterly monsoon drives the KBC northward through the Penghu Channel into the waters of southwestern Taiwan. When the northeasterly monsoon weakens as winter becomes summer (wet season, May–September), a southwesterly monsoon sets up, which forces the penetration of the SCSSC into the Taiwan Strait (TS) and gradually replaces the KBC. Thus, the current system should be stable in Taiwan Strait in summer. However, except for the above-mentioned succession of currents, the terrestrial runoff also influences the hydrographic conditions of the Gaoping waters. The terrestrial outflow from the Gaoping River (the largest river in southwestern Taiwan), particularly in the wet season, brings abundant nutrients into the Gaoping waters [33,34]. The high productivity supports the larval anchovy and benthic trawling fisheries [35,36], providing a spawning and nursery ground for many commercially fish taxa, such as Japanese butterfish (*Psenopsis anomala*), Shorthead anchovy (*Encrasicholina heteroloba*), Red bigeye (*Priacanthus macracanthus*), and True lizardfish (*Saurida undosquamis*).

Over the past two decades, a series of surveys studying the distribution, assemblage, growth, and vertical migration of mesopelagic fish larvae were carried out by the Japan Fisheries Research and Education Agency (FRA) on the onside of the Kuroshio off southern Japan, in the southern East China Sea, and in the transition region of the western North Pacific. For instance, in the southern East China Sea, Sassa and Konishi [37] reported that a northward intrusion of the Kuroshio transports mesopelagic fish larvae onto the continental shelf and competition for prey between mesopelagic and commercial pelagic fish larvae would potentially occur when the intrusion is strong. On the onshore side of the Kuroshio off southern Japan, Sassa and Hirota [6] found that the occurrence patterns of mesopelagic fish larvae are categorized into five seasonal groups in accordance to the local physical properties of the water column, suggesting that each species has a fixed seasonal pattern of reproduction. In addition, the various patterns of seasonal occurrence would result in seasonal habitat segregation of the larvae among species, potentially enabling the reduction of intraspecific competition for food resources in the oligotrophic waters of the Kuroshio. Sassa and Takahashi [38] compared the growth and mortality and their predatory impact on zooplankton of six mesopelagic larval taxa in the Kuroshio region off southern Japan. Their results show no significant difference in the ratio of growth coefficient/mortality coefficient among six mesopelagic larval taxa, and a consistent low level of predatory impact on zooplankton was suggested in the Kuroshio region. In contrast to the above-mentioned study areas, investigates of mesopelagic fish larvae in the Gaoping waters of southwestern Taiwan (even the waters surrounding Taiwan) are very scarce. In recent years, only Hsieh et al. [34] analyzed the spatiotemporal occurrences of mesopelagic fish larvae in relation to environmental forcing. They proposed that the distribution of

mesopelagic fish larvae was closely related to the hydrographic features, with surface temperature and mixed-layer depth being the major factors affecting the occurrence of mesopelagic fish larvae. Besides, the intrusion of the KBC played an important role in the transport of mesopelagic fish larvae from the Kuroshio region of eastern Taiwan into the Gaoping waters.

Although the mesopelagic fish larvae are usually dominant in the samples in our study area, no comprehensive evaluation of interannual changes under the different climatic conditions was made. We here examine large-scale climate influence (the Pacific Decadal Oscillation Index (PDO) and the Multivariate El Nino-Southern Oscillation Index (MEI)) on the physical and biotic environments (including seawater temperature, salinity, mixed layer depth, chlorophyll a concentration, and zooplankton abundance) and assemblage of summer mesopelagic fish larvae in the Gaoping waters from 2014 to 2018. The aims of the present study were to: (1) quantify differences in abundance and composition of summer mesopelagic fish larvae in the Gaoping waters between El Niño events (because the PDO exhibited positive values from September 2014 to May 2016, here we defined that the years 2015–2017 would be affected by El Niño events) and regular years (2014 and 2018); and (2) explore the relationships between fish larvae data and both large-scale climatic indices and local environmental variables. The contrasting hydrographic conditions of the Gaoping waters between El Niño events and regular years inspired our hypothesis that the varying marine environment would cause distinct assemblage structure of summer mesopelagic fish larvae between these two periods.

2. Materials and Methods

2.1. Field Sampling Work

Fish larvae and seawater samples were collected at 12 sampling stations of three transects in the Gaoping waters of southwestern Taiwan (Figure 1) during five summer cruises on board an RV Ocean Researcher III: OR3-1790 (22–24 August 2014, hereafter 2014), OR3-1877 (18, 19 August 2015, hereafter 2015), OR3-1957 (22–24 September 2016, hereafter 2016), OR3-2005 (8, 9 June 2017, hereafter 2017), and OR3-2066 (11, 12 June) and OR3-2072 (30, 31 July 2018, hereafter 2018). The three transects from north to south are located in Kaohsiung Harbor (hereafter KH), Gaoping River estuary (hereafter GR, a submarine canyon system), and Fengshan Township (hereafter FS), respectively. A 1.6 m mouth diameter Ocean Research Institute (ORI) net with a mesh size of 330 μm was used to sample fish larvae day and night. A mechanical flowmeter (Hydro-Bios, Kiel, Schleswig-Holstein, Germany) was placed centrally in the mouth opening to estimate the volume of filtered seawater. Tows were oblique at a speed of 1 m s^{-1} from the surface down to 100 m depth or 10 m above the bottom at shallow stations. The volume of water filtered in each station ranged from 21 to 877 m^3. Subsequently, all organisms collected were fixed and stored with 95% ethanol.

Hydrographic samplings (temperature, salinity, and fluorescence profiles) were performed at each station using a General Oceanic SeaBird conductivity-temperature-depth (CTD) meter (SEB-911 Plus, Bellevue, Washington, DC, USA) down to 100 m depth or 5 m above the bottom at shallow stations.

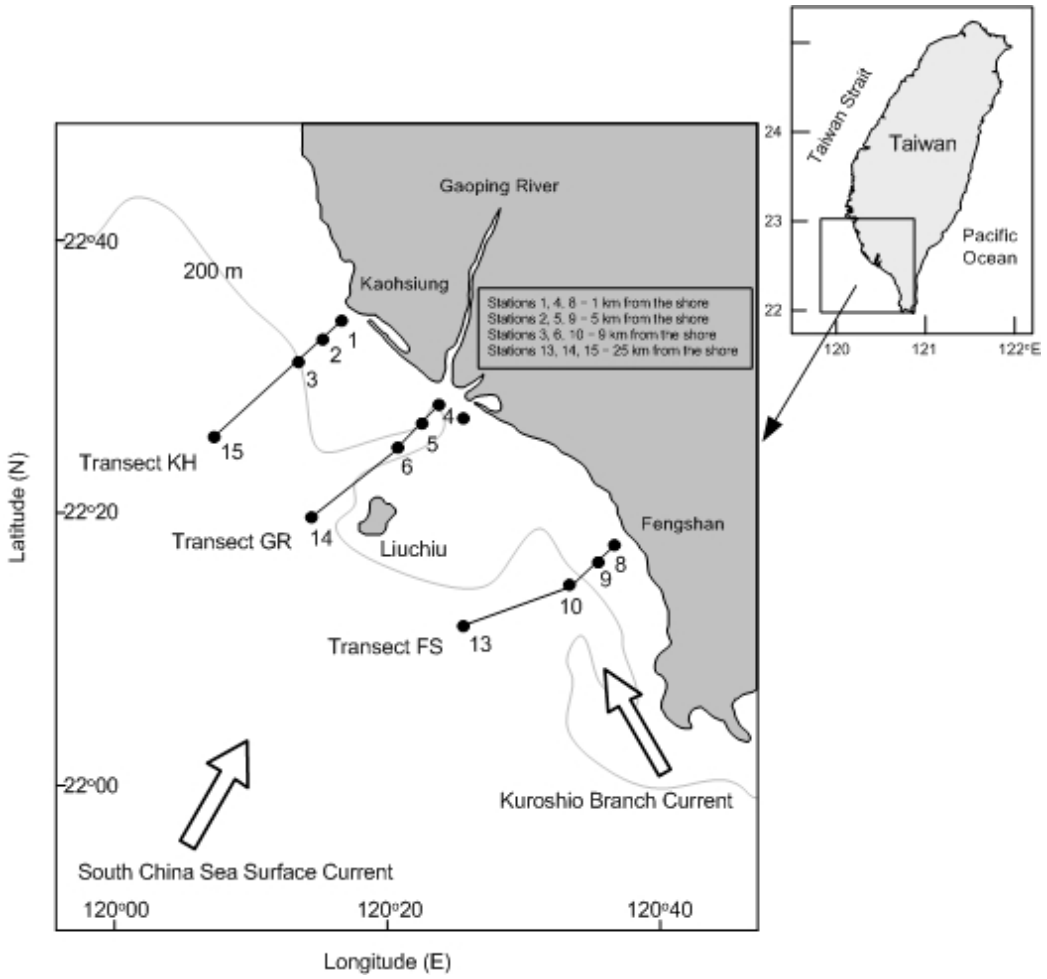

Figure 1. Map of the study area and sampling stations in the Gaoping coastal waters.

2.2. Laboratory Work

In the laboratory, all fish larvae were sorted and preserved in 95% ethanol after sorting. The mesopelagic fish larvae were sorted and identified to the lowest possible taxonomic level according to Leis and Rennis [39], Ozawa [40], Okiyama [41], Leis and Trnski [42], and Neira et al. [43]. The abundance of fish larvae was standardized to the number of individuals under 10 m^2 of sea surface using the volume of water filtered by the net and the maximum depth to which the net sampled.

$$A = N \div \left(\pi \times r^2 \times n \times 0.3\right) \times D \quad (1)$$

where A is abundance, N is the individuals of fish larvae, r is the radius of zooplankton net, n is the revolution of flowmeter, 0.3 is the coefficient of flowmeter, and D is the maximum sampling depth, respectively.

Once fish larvae were sorted, the remaining sample was divided into two subsamples using a Folsom plankton splitter (Aquatic Research Instruments, Wellington, New Zealand) to estimate zooplankton abundance. Repeated subsampling was taken until the number of individuals remaining in the last subsample was 1000–2000 or fewer. Going by the zooplankton classification of the Kuroshio waters [44], 33 zooplankton taxonomic groups were subsequently identified. Zooplankton abundance was expressed as the number of individuals per 1 m^3.

2.3. Data Analysis

The Shannon-Wiener diversity index (H') [45] and Pielou's evenness index (J') [44] were calculated to assess the diversity of the mesopelagic fish larvae in the samples. Analysis of variance (one-way ANOVA) [46] was used to determine the significance of differences between El Niño events and regular years in environmental (temperature, salinity, and mixed layer depth) and biotic variables (chlorophyll and zooplankton) and abundance and diversity of mesopelagic fish larvae. The mixed layer depth was defined as the depth from the seawater surface to the maximum depth where the temperature was almost the same as the surface temperature (±1 °C). Statistical significance was determined at $\alpha = 0.05$. If the result of ANOVA indicated that significant treatment effects were at the 0.05 probability level (P), then the post hoc Tukey's honestly significantly difference test was applied to determine which means differed significantly.

In order to observe the temporal difference in the assemblage structure of summer mesopelagic fish larvae, multivariate analyses were performed with the PRIMER-6 software package (PRIMER-E, West Hoe, Plymouth, UK). Data on larval abundance were $\log(x + 1)$-transformed to reduce the weighting of the dominant species. Similarity matrices of abundance of mesopelagic fish larvae in each sampling time were constructed using the Bray-Curtis Index [47]. These matrices were then employed to create a hierarchical agglomerative clustering using complete linkage to delineate groups with distinct community structure. In addition, non-metric multi-dimensional scaling (nMDS) [48] was also used to provide a two-dimensional visual representation of assemblage structure. Only 13 taxa with more than 1% of the total catch were included in the analysis avoiding any undue influence of rare species. Ordination scores produced by the nMDS were compared to local environmental variables (temperature, salinity, mixed layer depth, chlorophyll a, and zooplankton) using multiple regression analysis in order to determine which variables were significantly related to the larval assemblage structure [48,49]. In the regression analysis, the nMDS scores were treated as the independent variables and each environmental variable as the dependent variable. The rationale for selecting this method is described in Somarakis et al. [50]. Regression lines and their directions were plotted in the nMDS diagram according to Kruscal and Wish [48]. The direction of maximum correlation of each regression line is at an angle φ_r with the rth nMDS axis. The direction cosine (or regression weight) c_r of that angle is given by the following formula:

$$c_r = b_r / \sqrt{b_1^2 + b_2^2}, \quad (2)$$

where b_1 and b_2 are the coefficients from the multiple regression $a + b_1x_1 + b_2x_2$, and x_1 and x_2 are the scores in the first and second MDS axis, respectively.

Distance-based linear models (DistLM) [51] (one program of the multivariate statistical software of PERMANOVA+ for PRIMER, PRIMER-E (West Hoe, Plymouth, UK)) was applied to assess the relationship between assemblage structure of summer mesopelagic fish larvae and large-scale climatic indices. Two large-scale climatic indices were examined: the Pacific Decadal Oscillation Index (PDO) [52] obtained from JISAO, University of Washington and the Multivariate El Nino-Southern Oscillation Index (MEI) [53] from the NOAA Earth System Research Laboratory. Values in February–May, June–September, and October–January were averaged to indicate seasonal status in winter-spring, summer, and autumn–winter, respectively. Seasonal averages, with lags of up to one year, were used to account for delayed effects between physics and biology. These models were constructed using the stepwise selection procedure with the adjusted R^2 as the selection criterion. A similarity matrix of $\log(x + 1)$-transformed abundance of mesopelagic fish larvae in each sampling times was constructed using the Bray-Curtis Index. Finally, the full model was visualized by examining the distance-based redundancy analysis (dbRDA) to perform a constrained ordination of fitted values from the given multivariate regression model [54].

3. Results

3.1. Climatic and Hydrographic Conditions

Large-scale climatic indices (PDO and MEI) showed marked variations over the period of 2013–2019 (Figure 2). Fluctuation in PDO exhibited an alternate pattern between El Niño and La Niña events, in which a strong El Niño condition with positive values is shown from September 2014 to May 2016. The MEI displayed a similar variation trend, more pronounced El Niño condition occurred from May 2015 to January 2016. Our findings showed that the average seawater temperature of the 0–100 m water column (or 5 m above the bottom at shallow stations) throughout the study area ranged from 24.46 to 29.66 °C. No significant interannual difference in seawater temperature (ANOVA, $F = 1.668$, $p = 0.172$) was observed. Average salinity of the 0–100 m water column fluctuated between 28.78 and 34.44. No significant interannual difference in salinity (ANOVA, $F = 1.252$, $p = 0.301$) was found as well. Relatively lower salinity waters were generally recorded at stations within <1 km from the shore due to the inflows of freshwater, particularly on transects KH and GR.

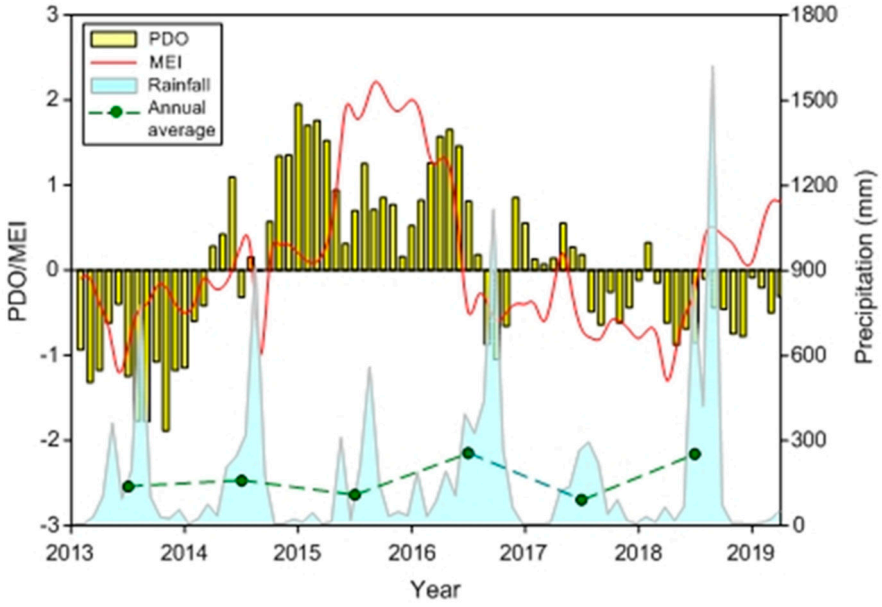

Figure 2. Time series of the Pacific Decadal Oscillation (PDO), Multivariate ENSO Index (MEI), and precipitation during 2013–2019. Data are based on monthly average for PDO and MEI and monthly accumulation and annual average for rainfall (rainfall data from Central Weather Bureau of the Republic of China).

On the other hand, regarding the vertical profiles of seawater temperature and salinity between 0 and 100 m water column recorded at station 6 (water depth of 282 m, 9 km from the shore), we noted a different phenomenon compared with the above-mentioned results. The water column at station 6 presented different conditions among years (Table 1, Figure 3). A thermocline was coupled with a strong halocline, separating the upper 40 m of the water column from the colder and more saline deeper layer in 2014 and 2018 (regular years). In contrast, the vertical structure of water was relatively well mixed in 2015–2017 (during and after El Niño events), particularly in 2016 with a mixed layer depth of 79 m (Table 1). Seawater temperature in the upper 100 m during and after El Niño events was about 5 °C higher than in regular years. In contrast to temperature, salinity showed an opposite phase. Mean values of salinity increased sharply from the surface to 10 m depth and were higher in regular years (Figure 3). During and after El Niño events salinity in the upper 100 m was about 1 salinity unit lower than in regular years due to the higher precipitation and relatively well water mixing.

Table 1. Comparisons of precipitation (14 days before sampling) and mixed layer depth, mean values of temperature, salinity, and chlorophyll a concentration (over the 0–100 m water column), and zooplankton abundance at station 6 during the study period.

Variable	Aug. 2014	Aug. 2015	Sep. 2016	Jun. 2017	Jun./Jul. 2018
Precipitation (mm)	902	548	1098	256	835/410
Mixed layer depth	18	25	79	28	24
Temperature (°C)	24.52 ± 2.90	26.69 ± 1.10	28.50 ± 0.67	27.32 ± 1.43	24.46 ± 3.36
Salinity	34.15 ± 0.57	34.14 ± 0.31	33.48 ± 0.26	33.82 ± 0.20	34.32 ± 0.23
Chlorophyll a (μg L^{-1})	0.20 ± 0.20	0.14 ± 0.03	0.26 ± 0.14	0.17 ± 0.07	0.37 ± 0.47
Zooplankton (individuals m^{-3})	648	624	402	302	2037

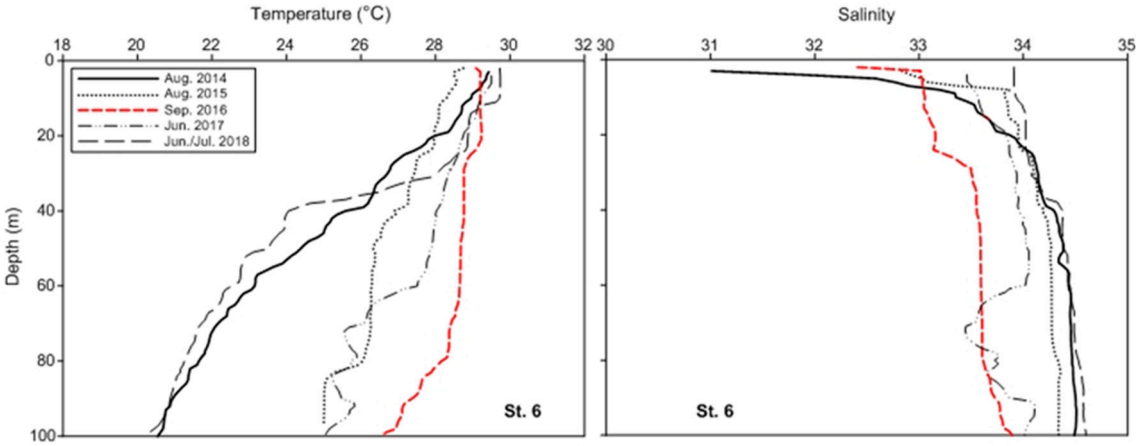

Figure 3. Vertical profiles of temperature and salinity between 0 and 100 m at station 6 during the study period.

3.2. Biological Variables

The overall concentration of chlorophyll a (mean ± SE) of the 0–100 m water column was 0.57 ± 0.11 μg L^{-1}, ranging from 0.08 to 3.52 μg L^{-1}. Chlorophyll a concentration showed significant interannual difference (ANOVA, F = 4.097, $p < 0.01$), with the highest average value in 2018 (1.15 ± 0.29 μg L^{-1}) and the lowest in 2015 (0.57 ± 0.11 μg L^{-1}). Higher chlorophyll a concentration usually occurred at stations within <1 km from the shore.

Zooplankton abundance varied from 9 to 3286 individuals (ind.) m^{-3}, with an over mean of 649 ± 83 (SE) ind. m^{-3}. Although zooplankton showed no significant difference among years (ANOVA, F = 1.750, $p = 0.153$), a slightly higher abundance was noted during and after El Niño events. In general, the distribution of zooplankton abundance was similar to that of the chlorophyll a concentration, usually with a higher abundance at the inshore stations. However, abundance of zooplankton should be considered as an underestimate due to the larger mesh size of zooplankton net.

3.3. Composition of Summer Mesopelagic Fish Larvae

A total of 1907 mesopelagic fish larvae were collected in the study, in which 75 taxa or morphotypes were identified belonging to 9 families and 31 genera. The majority of larvae were identified as being in the preflexion stage (1373 individuals, ca. 72%). Larvae of the families Myctophidae, Gonostomatidae, Paralepididae, and Stomiidae were the most abundant and accounted for 77.3, 12.4, 7.1, and 2.4% of the total larval catch, respectively. Among them, Myctophidae had the largest number of species (38 taxa), followed by Paralepididae (13 taxa), Gonostomatidae, and Stomiidae (8 taxa each). At the species level, *Benthosema pterotum* was the most dominant taxon (31.2%) in the study. The other predominant taxa (>1% of the total catch) were *Diaphus* slender type (19.9%), *Cyclothone alba* (7.2%), *Diaphus* stubby type (5.9%), *Vinciguerria nimbaria* (4.4%), *Diaphus richardsoni* (3.3%), *Hygophum proximum* (2.4%), *Cyclothone pseudopallida* (2.2%), *Benthosema fibulatum*

(2.1%), *Lampanyctus nobilis* (2.1%), *Cyclothone* spp. (1.7%), *Myctophum orientale* (1.2%), and *Ceratoscopelus warmingii* (1.0%). These 13 taxa together constituted 84.5% of the total catch collected during the study period.

3.4. Interannual Differences in Abundance and Diversity of Summer Mesopelagic Fish Larvae

The overall mean abundance of summer mesopelagic fish larvae (mean ± SD) was 145 ± 228 ind. 10 m^{-2}. Abundance of summer mesopelagic fish larvae showed apparent difference among years (ANOVA, F = 3.033, $p < 0.05$). Higher mean abundance was recorded in 2017 (264 ± 407 ind. 10 m^{-2}), moderate abundance was seen in 2015 (182 ± 129 ind. 10 m^{-2}), and lower abundances were observed in 2014 (53 ± 54 ind. 10 m^{-2}), 2016 (33 ± 31 ind. 10 m^{-2}), and 2018 (46 ± 69 ind. 10 m^{-2}) (Figure 4). Due to the high abundance of one predominant species, *Benthosema pterotum*, one peak abundance was recorded at station 9 in 2017. Summer mesopelagic fish larvae were always abundant at stations >5 km from the shore and scarce or absent at stations within <1 km from the shore throughout the study period.

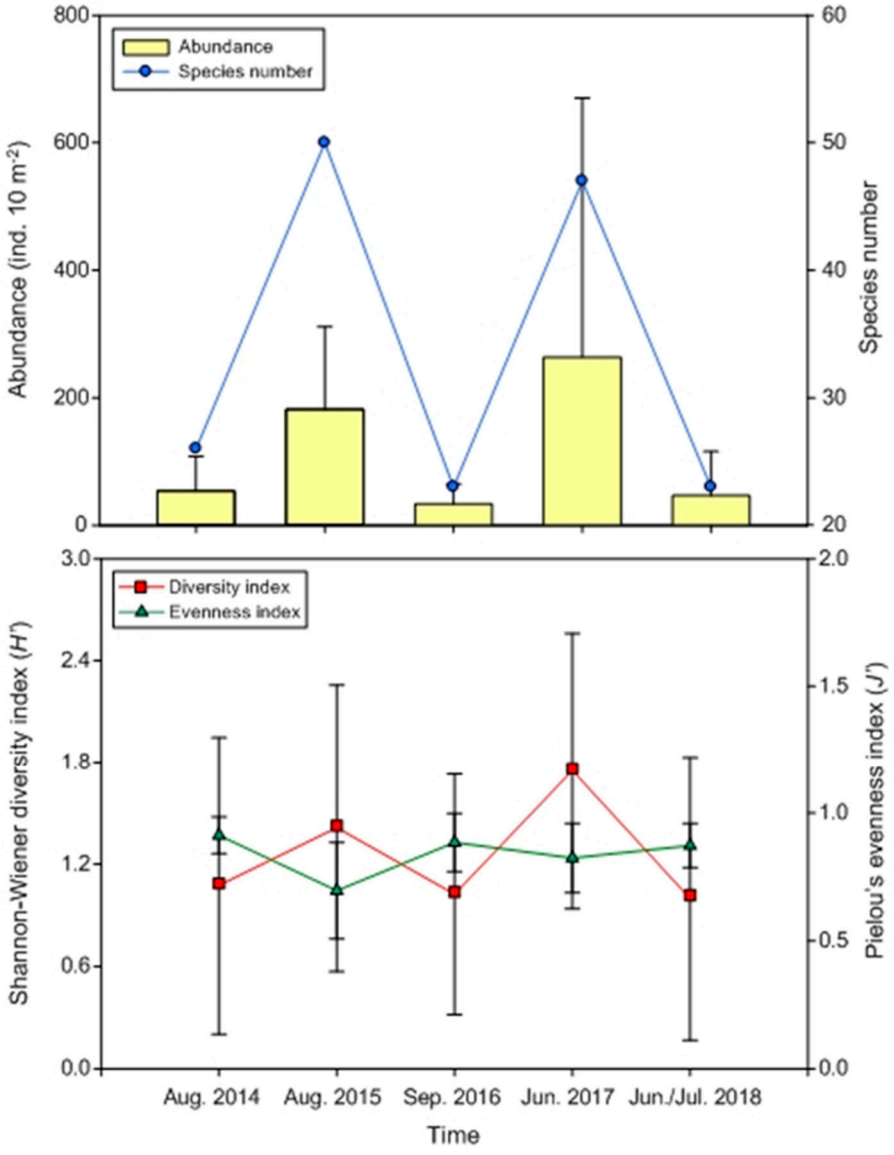

Figure 4. Species number and mean values (±SD) of abundance, Shannon-Wiener diversity index (H', loge), and Pielou's evenness index (J') of mesopelagic fish larvae in the Gaoping waters off southwestern Taiwan during the study period.

The variation patterns of the species number and Shannon-Wiener diversity index consist with abundance (Figure 4). Significant interannual difference was found in species number (ANOVA, F = 5.308, $p < 0.01$), but not in Shannon-Wiener diversity index (ANOVA, F = 1.822, $p = 0.139$). The number of species was greater in 2015 (50) and 2017 (47) than in 2014 (26), 2016 (23), and 2018 (23). Both species number and Shannon-Wiener diversity index, in general, increased with increasing distance from the shore, most likely due to the bottom depth. The interannual variation in Pielou's evenness index showed an opposite trend to those of species number and Shannon-Wiener diversity index (Figure 4), with lower mean values in 2015 and 2017. Similarly, higher values of Pielou's evenness index were observed in the offshore stations. There was a significant difference in Pielou's evenness index among years (ANOVA, F = 4.035, $p < 0.01$).

When examining interannual trends in abundance (Table 2, Figure 5), it was quite evident that certain dominant taxa exhibited contrasting patterns between El Niño events and regular years. For example, *Benthosema pterotum*, which was the most abundant species, had significantly higher abundances in 2015 and 2017 and lower in 2016. A similar pattern was observed for two types of the genus *Diaphus*. With the exceptions of two species, *Cyclothone alba* and *Benthosema fibulatum* presented relatively increased abundances during and after El Niño events. Besides, larvae of *Vinciguerria nimbaria*, *Lampanyctus nobilis*, and *Myctophum orientale* showed significantly lower abundance (or absence) in El Niño events than in regular years.

Table 2. Mean abundance (individuals 10 m^{-2}) of dominant mesopelagic fish larvae (relative abundance > 1%) in the Gaoping waters off southwestern Taiwan during the study period.

Family/Taxon	Aug. 2014	Aug. 2015	Sep. 2016	Jun. 2017	Jun./Jul. 2018	N (Count of Individuals)	Percentage of the Total Catch (%)
Gonostomatidae							
Cyclothone alba	6.2	1.3	14.9	15.7	3.6	115	7.2
C. pseudopallida	1.8	0.7	1.0	8.9	–	40	2.2
Cyclothone spp.	0.4	3.7	2.2	3.2	0.5	30	1.7
Myctophidae							
Benthosema fibulatum	–	–	3.2	9.1	–	14	2.1
B. pterotum	1.7	60.1	2.2	105.5	9.8	290	31.2
Ceratoscopelus warmingii	0.8	0.8	1.3	2.4	0.5	19	1.0
Diaphus richardsoni	–	1.2	–	17.4	–	47	3.3
Diaphus slender type	12.2	64.5	1.8	22.5	15.4	287	19.9
Diaphus stubby type	5.4	16.1	0.6	10.9	0.5	81	5.9
Hygophum proximum	0.3	0.5	0.6	12.5	–	24	2.4
Lampanyctus nobilis	5.1	0.8	–	4.7	1.7	29	2.1
Myctophum orientale	0.8	1.2	–	4.3	0.5	15	1.2
Phosichthyidae							
Vinciguerria nimbaria	8.8	4.3	1.3	6.8	5.1	60	4.4

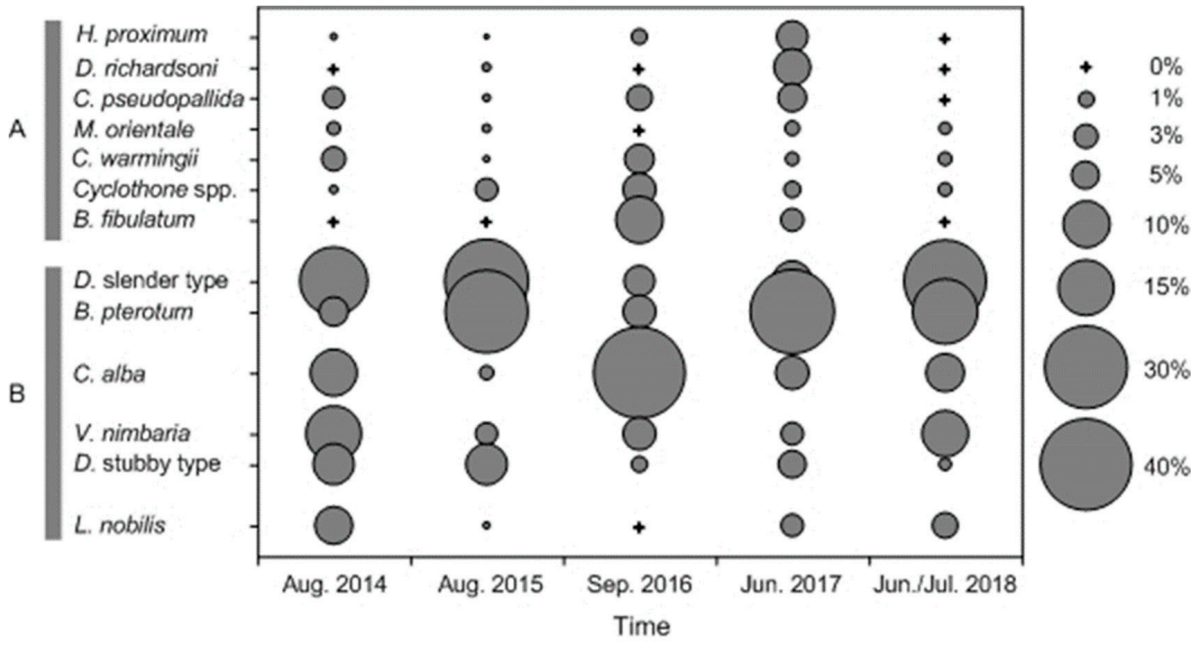

Figure 5. Occurrence patterns of the 13 dominant mesopelagic fish larvae in the Gaoping waters off southwestern Taiwan in five summers during 2014–2018. Each bubble is the relative abundance, expressed as a percentage of the total catch. Groups (**A**, **B**) were named according to Figure 6.

3.5. Species Groups of Summer Mesopelagic Fish Larvae

Two significant species groups were detected by cluster analysis based on Bray-Curtis similarity matrix of log(x + 1)-transformed abundance of 13 dominant mesopelagic fish larvae (with a relative abundance > 1%) (Figure 6). Group A was composed of seven taxa: two gonostomatid taxa (*Cyclothone pseudopallida* and *Cyclothone* spp.) and five myctophid species (*Hygophum proximum*, *Diaphus richardsoni*, *Myctophum orientale*, *Ceratoscopelus warmingii*, and *Benthosema fibulatum*). These larval taxa usually had higher abundances in 2017 after the strong El Niño events, and parts of them were scarce or absent in regular years (Table 2). Although this group was characterized by lower abundance, it had a broad distribution throughout the study period. Group B consisted of larvae of four myctophid species (*Benthosema pterotum, Diaphus* slender type, *Diaphus* stubby type, and *Lampanyctus nobilis*), one phosichthyid species (*Vinciguerria nimbaria*), and one gonostomatid species (*Cyclothone alba*). Among the six taxa, significantly higher abundances of larvae of *Benthosema pterotum, Diaphus* slender type, *Diaphus* stubby type, and *Vinciguerria nimbaria* were observed in 2015 and 2017 and significantly lower in 2014, 2016, and 2018 (Table 2). These taxa were usually abundant at stations >5 km from the shore. *Cyclothone alba* showed relatively higher abundances in 2016 and 2017 and lower in 2015. Abundance of larvae of *Lampanyctus nobilis* was scarce or absent in 2015, 2016, and 2018 and relatively higher in 2014 and 2017.

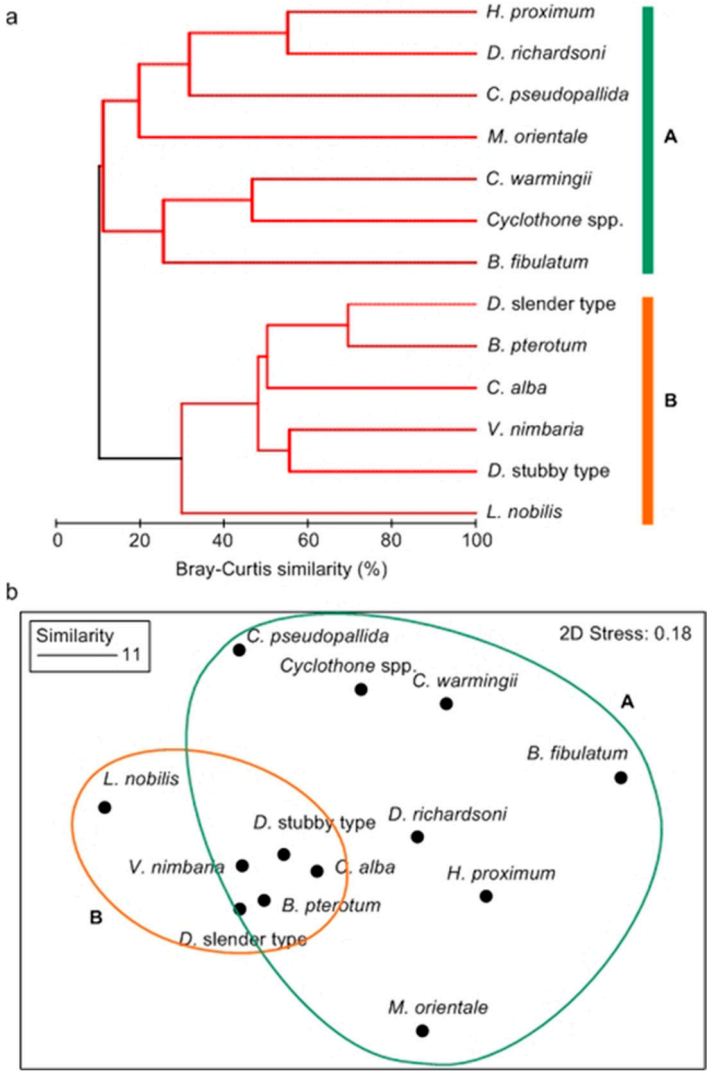

Figure 6. (**a**) Dendrogram showing the classification of the occurrence patterns of the 13 dominant mesopelagic fish larvae based on the Bray-Curtis similarity of each species taxa. The clusters with dotted lines denote a significant difference in occurrence times among cluster groups (similarity profile (SIMPROF) test, $p < 0.05$). (**b**) Ordination plot of comparison of species using non-metric multidimensional scaling (nMDS).

3.6. Summer Mesopelagic Fish Larvae Assemblage in Relation to Environmental Variables

The result of nMDS based on similarity matrix of log(x + 1)-transformed abundance of 13 dominant taxa showed that samples were differentiated mainly according to temperature but also according to the regular-warm regime (Figure 7). Seawater temperature, salinity, and chlorophyll a explained 22.1%, 18.1%, and 15.8% of the variation in the ordination (Table 3), along the axis separating the regular years and during and after El Niño events (Figure 7).

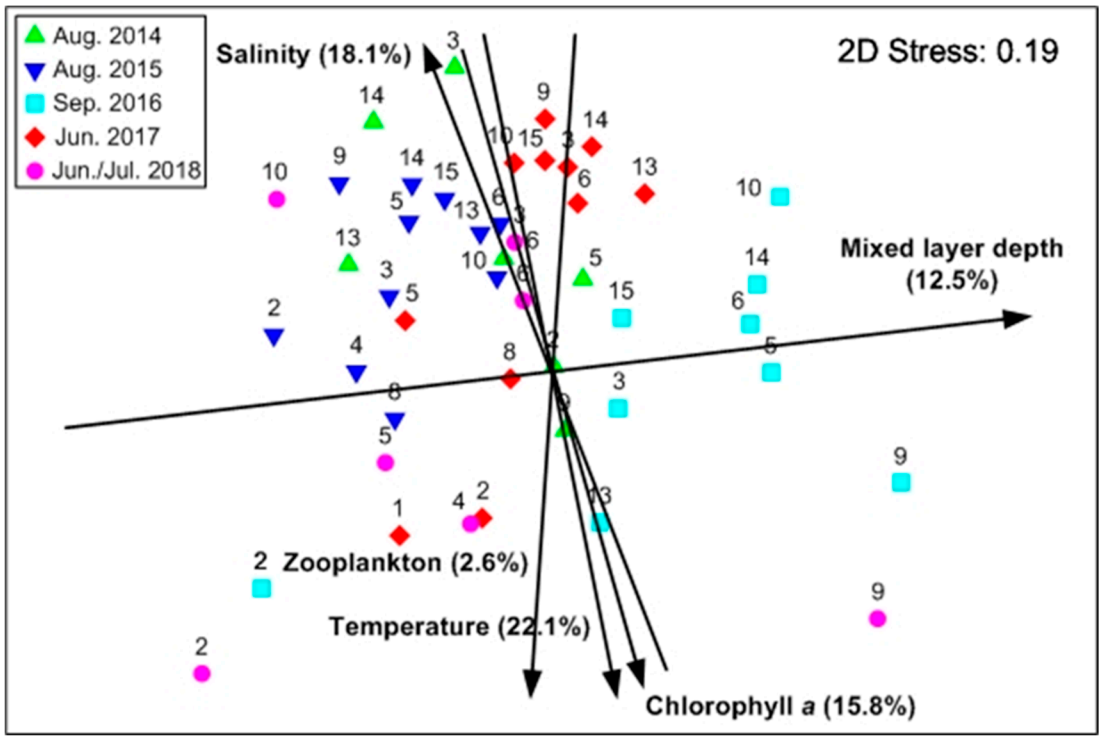

Figure 7. Non-metric multidimensional scaling (nMDS) ordination of the station groups based on Bray-Curtis similarity matrix of log(x + 1)-transformed abundance of 13 dominant mesopelagic fish larvae. Significant multiple regressions between ordination scores and environmental parameters are shown, as well as the fraction (%) of variance explained (see Table 3). Regular years: 2014 and 2018; during and after El Niño event: 2015–2017.

Table 3. Multiple regression analysis between environmental parameters (temperature, salinity, and chlorophyll a concentration (over the sampling water column), mixed layer depth, and zooplankton abundance) and nMDS scores for two-axis ordination of sampling stations. X and Y: direction cosines.

Variable	X	Y	R^2	F	P
Temperature	0.14	−0.99	0.221	5.947	0.005 **
Salinity	−0.41	0.91	0.181	4.648	0.015 *
Mixed layer depth	0.98	0.18	0.125	3.011	0.060
Chlorophyll a	0.23	−0.97	0.158	3.941	0.027 *
Zooplankton	−0.09	−0.99	0.026	0.563	0.574

** <0.01, * <0.05.

DistLM analysis was used to examine the relationship between assemblage structure of summer mesopelagic fish larvae and PDO and MEI indices. The first and second dbRDA axes captured 42.9% and 30.8% of the variance in the fitted model, which corresponded to 12.2% and 8.8% of the total variance in the original Bray-Curtis similarity matrix (Figure 8). All eight PDO and MEI variables, considering the delayed effects between physics and biology, together explained 19.91% of the total variation (Table 4). No significant explanatory variables that can explain the pattern were found in the assemblage structure of summer mesopelagic fish larvae in the Gaoping waters between El Niño events and regular years.

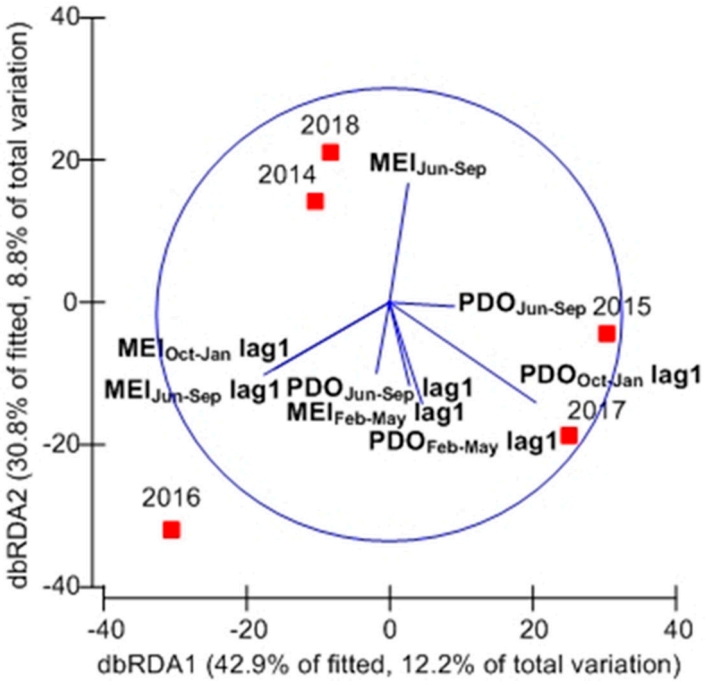

Figure 8. Distance-based redundancy analysis (dbRDA) ordination for the composition of mesopelagic fish larvae constrained by the PDO and MEI indices. PDO: Pacific Decadal Oscillation Index; MEI: Multivariate El Nino-Southern Oscillation Index.

Table 4. Percentage of variation in assemblages of summer mesopelagic fish larvae explained by PDO (Pacific Decadal Oscillation Index) and MEI (Multivariate El Nino-Southern Oscillation Index) indices included in the distance-based linear models for sampling times.

Variables	SS (Trace)	Pseudo-F	P	% Variation Explained
$PDO_{Jun.-Sep.}$	1337.5	0.796	0.702	2.09
$PDO_{Feb.-May}$ × lag1 (lag of up to one year)	1497.6	0.920	0.570	2.34
$PDO_{Oct.-Jan.}$ × lag1	1591.7	0.997	0.549	2.49
$PDO_{Jun.-Sep.}$ × lag1	1467.5	0.896	0.655	2.30
$MEI_{Jun.-Sep.}$	1398.4	0.842	0.591	2.19
$MEI_{Feb.-May}$ × lag1	1454.5	0.886	0.551	2.28
$MEI_{Oct.-Jan.}$ × lag1	1965.3	1.336	0.245	3.08
$MEI_{Jun.-Sep.}$ × lag1	2004.9	1.375	0.249	3.14

4. Discussion

The summer mesopelagic larval assemblages in the Gaoping waters were dominated by a few taxa, e.g., *Benthosema pterotum*, *Diaphus* slender type, *Diaphus* stubby type, *Cyclothone alba*, and *Vinciguerria nimbaria*. On average, the abundances of these larvae, except *Cyclothone alba*, showed significant interannual changes, with low values in 2016 (the end of strong El Niño events). Besides, in 2016, the seawater temperature in the upper 100 m and precipitation was exceptionally high. We speculated that these conditions would limit the biological production in the study area, negatively affecting the abundance and survival of mesopelagic fish larvae.

In fact, the influence of the El Niño on Taiwan is not very obvious. Studies in Taiwan have found that during the El Niño events, the temperature in the summer of that year is relatively low, the following winter is relatively warm, the next year has more spring rain, and the temperature in summer is also relatively high [55]. Generally, the summer hydrography in the Gaoping waters was mainly influenced by the monsoon-driven current

system and terrestrial runoff [31,33]. During this period, the warm and low-salinity SCSSC flows northeastward, synchronizing with the southwesterly monsoon, intruding into the TS and dominating this region [31,32]. Meanwhile, the high-temperature and high-salinity KBC intrudes into the northern SCS. These oceanographic conditions led to higher seawater temperatures at the northern SCS and the Gaoping waters [34]. This could be revealed by the high average seawater temperatures of the 0–100 m water column, usually >27 °C, observed throughout the survey area in the present study.

Large-scale climate change in the North Pacific likely affects the surface current and water features in the TS via oceanic physical processes [56,57]. In general, key features of composite positive MEI events (warm, El Niño) include: (1) anomalously warm sea surface temperature (SST) across the east-central equatorial Pacific; (2) anomalously high sea level pressure (SLP) over Indonesia and the western tropical Pacific and low SLP over the eastern tropical Pacific; (3) reduction of tropical Pacific easterly winds (trade winds); and (4) suppressed tropical convection over Indonesia and Western Pacific and enhanced convection over the central Pacific. Among these features, changes in SLP are closely associated with changes in trade winds, which are an important component of ocean-atmosphere interaction and heat exchange. Changes of wind will affect the variability in the sea surface temperature, upper ocean temperature, mixed layer depth, and direction and strength of near surface wind-driven currents directly [58,59].

The El Niño events have been suggested to cause strong southwesterly winds over the western North Pacific in the summer [60]. According to the empirical orthogonal function analysis on the long-term summertime SST data of the TS during 1982–2012 [59], a warming trend in the TS was observed with the spatially average warming of 0.057 °C y^{-1} and an interannual variation in the SST was found after 1994, which was strongly correlated with the wind speed of the southwesterly monsoon. Strengthening winds enhanced the upwelling along the China coast, eastern Taiwan Banks, and the region south of Peng-Hu Islands, whereas the SST in eastern TS increased because of the increased transport of warm SCSSC. Although no southwesterly monsoon information was collected in this study, the significant differences in seawater temperature, salinity, and mixed layer depth of the upper 100 m at station 6 between El Niño events and regular years were noted (Table 1, Figure 3). We thought that the strengthening southwesterly monsoon during El Niño events enhanced the seawater vertical mixing and warmed the upper ocean temperature indirectly.

In the subtropical waters, increased mixing reduces stratification which tends to increase phytoplankton production due to a rise in surface nutrient concentration. Nevertheless, this phenomenon in our study was not significant even if an apparent seawater mixing increase was recorded during and after El Niño events. In contrast to the increase of upper layer nutrients levels through mixing, terrestrial outflow is the main source of nutrients in the Gaoping waters [33,34]. Plentiful nutrients have entrained higher phytoplankton production, which were the food resources for grazers such as copepods and their predators, such as gelatinous carnivores and fish larvae [61–63]. However, climate-associated fluctuations in the timing and amount of precipitation influence river discharge, which in turn affects the entrainment of nutrients and the magnitude of phytoplankton production [21,64]. The composition of phytoplankton community can be changed by the entrained nutrients. Furthermore, variation in the intensity of seasonal monsoon can also alter the timing of the phytoplankton bloom in the TS [65]. Taken together, these factors all contribute to the survival and growth of zooplankton and further influence the distribution and occurrence of mesopelagic fish larvae in the Gaoping waters.

Several previous studies on the continental shelf of the Northeast Pacific and in the northwestern Mediterranean have linked large-scale climate forcing factors to variations in larval abundances of oceanic commercial fish. For example, in the southern California Current region, Hsieh et al. [27] found that variations in the abundance of most oceanic fish species have a significant correlation with environmental factors, which is consistent with the change trend of the PDO. Using generalized additive models, Auth et al. [66] observed

that large-scale climate indices, particularly the PDO, explain more variability in fish larvae abundance than local environmental factors did. In the Strait of Georgia, Guan et al. [30] proposed that large-scale climate processes are potential contributions to variations in overall larval concentrations of the dominant taxa and assemblage composition. Raya and Sabatés [67] also reported significantly low abundance of carangid fish larvae in July 2003 when the European region suffered an exceptional heat wave with air temperature records of about 3–6 °C above the seasonal average. However, in the present study, the fluctuations in abundance and composition of summer mesopelagic fish larvae assemblage were not affected directly by changes in large-scale climatic conditions (Figure 8).

According to the directions of summer currents in the TS [31], we speculated that there are three possibilities for the origin of these mesopelagic fish larvae occurring in the Gaoping waters: (1) they were spawned in the study area; (2) transport from the South China Sea into the surface layer of the southern TS by the SCSSC; and (3) transport from the Kuroshio region of eastern Taiwan into the mesopelagic layer of the Gaoping waters by the KBC. Generally, the mesopelagic fish larvae have a fixed seasonal pattern of reproduction, and no significant interannual differences occurred in the months of peak abundances of the larvae [6]. In the Kuroshio offshore waters off southwestern Kyushu Islands of Japan, Sassa et al. [7] and Sassa and Takahashi [38] also recorded the same six predominant taxa of mesopelagic fish larvae between February 1997 and 2010. These results indicated that the abundance and composition of the summer dominant mesopelagic fish larvae assemblage in the Gaoping waters seem to be stable. However, in this study it was quite evident that certain dominant taxa exhibited contrasting patterns between El Niño events and regular years. For instance, the predominant *Benthosema pterotum* and two types of genus *Diaphus* of the family Myctophidae showed significantly higher abundances in 2015 and 2017 and lower in 2016 (Table 2, Figure 5).

The results of nMDS analysis suggested a distinct occurrence pattern of summer mesopelagic fish larvae assemblage related to seawater temperature, salinity, and chlorophyll a concentration (Table 3, Figure 7). The best direct evidence of the effects of climate change on marine ecosystems most likely comes from distributional shifts of marine organisms [68]. Considering the habitat of mesopelagic adult-stage fishes, these species inhabit the deeper oceanic waters, and in the North Pacific their larvae are usually distributed in high salinity waters (>34) [7,17]. In this study, the abundance of mesopelagic fish larvae showed a significantly negative correlation with seawater temperature (linear regression, $t = -3.910$, $p < 0.001$) indicating the accumulation of mesopelagic fish larvae at the relatively low temperature station (with deeper bottom depth). In addition, they occurred mainly at the stations >5 km from the shore and scarce or absent at stations within <1 km from the shore. We speculated that despite the abundant food availability and the more mesopelagic fish larvae onto the Gaoping waters carried by the increased transport of the SCSSC (or KBC) during El Niño events, the higher temperature and lower salinity at the inshore upper waters might be unsuitable for mesopelagic fish larvae, possibly resulting in low egg and larval survival. Off the Georges Bank, Colton [69] reported mortality of large numbers of cod larvae, and concluded it was due to thermal shock caused by transport of the larvae off the Bank into much warmer Slope Water offshore.

Highly productive nature of estuarine and coastal waters and their role as spawning grounds (or nursery grounds) to fish are well known for temperate and tropical areas [70,71]. Since early the life stages of fish are a particularly vulnerable phase, it is hypothesized that marine fish larvae and juveniles migrate into estuarine and coastal waters to make use of the high food abundance and refuge against predators, in order to maximize survival [14]. In general, larvae of most mesopelagic fishes (e.g., myctophids) are less common below the thermocline than in or above it [14,72] and show species-specific distribution depths in the epipelagic layer [17,73]. Thus, the increased vertical distribution of natural food during El Niño events in the Gaoping waters would be favorable for mesopelagic fish larvae. We do know that climate variation would impact population dynamics of marine organisms indirectly through multi-step processes in food webs under “bottom-up” and “top-down”

controls [74–76]. In the Strait of Georgia, Canada, DiLorenzo et al. [77] and Mackas et al. [78] have evidenced that variations in the timing of the spring phytoplankton bloom and zooplankton biomass are significantly correlated with the North Pacific Gyre Oscillation index, which indicates fluctuations in the mechanisms driving plankton dynamics in the Northeast Pacific. In the southern East China Sea, Sassa and Tsukamoto [79] proposed that the between-year difference in habitat temperature and food availability would influence the larval growth of *Scomber japonicus* and *S. australasicus*. However, in our study, there is no significant difference in zooplankton abundance observed among survey years, but slightly higher zooplankton abundances were recorded during and after El Niño events. In addition, higher zooplankton abundances usually occurred at the inshore stations. Unfortunately, the occurrence of mesopelagic fish larvae did not correlate significantly with chlorophyll *a* concentration (linear regression, $t = -1.552$, $p = 0.126$) and zooplankton abundance (linear regression, $t = 1.012$, $p = 0.316$). These results seem to indicate that the variations of the inshore seawater temperature and salinity are more important than the availability and abundance of food resources in determining the distribution and survival of mesopelagic fish larvae, particularly at very early life stages when the yolk is exhausted [14,16]. Nevertheless, the error of an underestimate of zooplankton abundance due to larger mesh size of zooplankton net should be considered.

In conclusion, the results of the present study showed the interannual differences on the abundance and composition in summer mesopelagic fish larvae between El Niño events and regular years in the Gaoping waters. Large-scale climate change in the North Pacific influences the surface current and water features in the TS via oceanic physical processes. In this study, significantly higher seawater temperature, mixed layer depth, and lower salinity in the upper 100 m and higher precipitation were recorded at the end of the strong El Niño events (summer 2016). The strengthening southwesterly monsoon during El Niño events likely enhanced the seawater vertical mixing and warmed the upper ocean temperature indirectly. Although the abundance and composition of mesopelagic fish larvae assemblage were not affected directly by changes in large-scale climatic conditions, the occurrence of mesopelagic fish larvae was related to seawater temperature, salinity, and chlorophyll a concentration. We speculated that despite the abundant food availability and the more mesopelagic fish larvae onto the Gaoping waters transported by the increased inflow of the South China Sea Surface Current during El Niño events, the higher temperature and lower salinity at the inshore upper waters might be unsuitable for mesopelagic fish larvae, possibly resulting in low egg and larval survival. These results have not only expanded our knowledge on the occurrence of summer mesopelagic fish larvae in the Gaoping waters, but has also provided good examples of biotic responses to the large-scale climate change.

Author Contributions: Formal analysis, C.-C.L.; funding acquisition, H.-Y.H.; investigation, H.-Y.H., W.-T.L. and C.-C.L.; methodology, H.-Y.H., W.-T.L. and C.-C.L.; supervision, P.-J.M.; writing—original draft, P.-J.M.; writing–review and editing, H.-Y.H. All authors have read and agreed to the published version of the manuscript.

Funding: This research is funded by the Ministry of Science and Technology of the Republic of China to H.-Y. Hsieh (MOST 103-2611-M-259-003, MOST 104-2611-M-259-001, MOST 105-2611-M-259-001 and MOST 106-2611-M-259-001).

Institutional Review Board Statement: Not applicable.

Acknowledgments: We deeply appreciate the crew of the Ocean Researcher III for their assistance in collecting zooplankton samples and environmental data. No specific permissions were required for the sampling locations and activities.

Conflicts of Interest: The authors declare no conflict of interest.

References

1. Sassa, C.; Kawaguchi, K.; Kinoshita, T.; Watanabe, C. Assemblages of vertical migratory mesopelagic fish in the transitional region of the western North Pacific. *Fish. Oceanogr.* **2002**, *11*, 193–204. [CrossRef]
2. Nelson, J.S.; Grande, T.C.; Wilson, M.V. *Fishes of the World*; John Wiley & Sons: Hoboken, NJ, USA, 2016.

3. Irigoien, X.; Klevjer, T.A.; Røstad, A.; Martinez, U.; Boyra, G.; Acuña, J.L.; Bode, A.; Echevarria, F.; Gonzalez-Gordillo, J.I.; Hernandez-Leon, S.; et al. Large mesopelagic fishes biomass and trophic efficiency in the open ocean. *Nat. Commun.* **2014**, *5*, 3271–3280. [CrossRef]
4. FAO. *FAO Yearbook: Fishery and Aquaculture Statistics. Capture Production 2011*; FAO: Rome, Italy, 2013.
5. Sabatés, A. Diel vertical distribution of fish larvae during the winter-mixing period in the Northwestern Mediterranean. *ICES J. Mar. Sci.* **2004**, *61*, 1243–1252. [CrossRef]
6. Sassa, C.; Hirota, Y. Seasonal occurrence of mesopelagic fish larvae on the onshore side of the Kuroshio off southern Japan. *Deep Sea Res. Part I Oceanogr. Res. Pap.* **2013**, *81*, 49–61. [CrossRef]
7. Sassa, C.; Kawaguchi, K.; Hirota, Y.; Ishida, M. Distribution patterns of larval myctophid fish assemblages in the subtropical-tropical waters of the western North Pacific. *Fish. Oceanogr.* **2004**, *13*, 267–282. [CrossRef]
8. Olivar, M.P.; Bernal, A.; Molí, B.; Peña, M.; Balbín, R.; Castellón, A.; Miquel, J.; Massutí, E. Vertical distribution, diversity and assemblages of mesopelagic fishes in the western Mediterranean. *Deep Sea Res. Part I Oceanogr. Res. Pap.* **2012**, *62*, 53–69. [CrossRef]
9. Williams, A.; Koslow, J.A.; Terauds, A.; Haskard, K. Feeding ecology of five fishes from the mid-slope micronekton community off southern Tasmania, Australia. *Mar. Biol.* **2001**, *139*, 1177–1192.
10. Cherel, Y.; Ducatez, S.; Fontaine, C.; Richard, P.; Guinet, C. Stable isotopes reveal the trophic position and mesopelagic fish diet of female southern elephant seals breeding on the Kerguelen Islands. *Mar. Ecol. Prog. Ser.* **2008**, *370*, 239–247. [CrossRef]
11. Davison, P.C.; Checkley, D.M.; Koslow, J.A.; Barlow, J. Carbon export mediated by mesopelagic fishes in the northeast Pacific Ocean. *Prog. Oceanogr.* **2013**, *116*, 14–30. [CrossRef]
12. Young, P.C.; Leis, J.M.; Hausfeld, H.F. Seasonal and spatial distribution of fish larvae in waters over the North West Continental Shelf of Western Australia. *Mar. Ecol. Prog. Ser.* **1986**, *31*, 209–222. [CrossRef]
13. Doyle, M.J.; Morse, W.W.; Kendall, A.W., Jr. A comparison of larval fish assemblages in the temperate zone of the northeast Pacific and northwest Atlantic Oceans. *Bull. Mar. Sci.* **1993**, *53*, 588–644.
14. Olivar, M.P.; Emelianov, M.; Villate, F.; Uriarte, I.; Maynou, F.; Álvarez, I.; Morote, E. The role of oceanographic conditions and plankton availability in larval fish assemblages off the Catalan coast (NW Mediterranean). *Fish. Oceanogr.* **2010**, *19*, 209–229. [CrossRef]
15. Olivar, M.P.; Beckley, L.E. Influence of the Agulhas Current on the distribution of lanterfish larvae off southeast coast of Africa. *J. Plankton Res.* **1994**, *16*, 1759–1780. [CrossRef]
16. Sabatés, A.; Olivar, M.P.; Salat, J.; Palomera, I.; Alemany, F. Physical and biological processes controlling the distribution of fish larvae in the NW Mediterranean. *Prog. Oceanogr.* **2007**, *74*, 355–376. [CrossRef]
17. Moser, H.G.; Smith, P.E. Larval fish assemblages and oceanic boundaries. *Bull. Mar. Sci.* **1993**, *53*, 283–289.
18. Shepherd, F.G.; Cushing, D.H. A mechanism for density-dependent survival of larval fish as the basis of a stock-recruitment relationship. *ICES J. Mar. Sci.* **1980**, *39*, 160–167. [CrossRef]
19. Takahashi, M.; Watanabe, Y. Growth rate-dependent recruitment of Japanese Anchovy *Engraulis japonicus* in the Kuroshio-Oyashio transitional waters. *Mar. Ecol. Prog. Ser.* **2004**, *266*, 227–238. [CrossRef]
20. Cheung, W.L.; Lam, V.Y.; Sarmiento, J.L.; Kearney, K.; Watson, R.; Pauly, D. Projecting global marine biodiversity impacts under climate change scenarios. *Fish Fish.* **2009**, *10*, 235–251. [CrossRef]
21. Drinkwater, K.F.; Beaugrand, G.; Kaeriyama, M.; Kim, S.; Ottersen, G.; IanPerry, R.; Pörtner, H.-O.; Polovina, J.J.; Takasukaj, A. On the processes linking climate to ecosystem changes. *J. Mar. Syst.* **2010**, *79*, 374–388. [CrossRef]
22. Ganias, K.; Somarakis, S.; Machias, A.; Koutsikopoulos, C. Factors affecting the spawning period of sardine in two highly oligotrophic Seas. *Mar. Biol.* **2007**, *151*, 1559–1569. [CrossRef]
23. Stratoudakis, Y.; Coombs, S.; de Lanzós, A.L.; Halliday, N.; Costas, G.; Caneco, B.; Franco, C.; Conway, D.; Santos, M.B.; Silva, A.; et al. Sardine (*Sardina pilchardus*) spawning seasonality in European waters of the northeast Atlantic. *Mar. Biol.* **2007**, *152*, 201–212. [CrossRef]
24. Bernal, M.; Stratoudakis, Y.; Coombs, S.; Angelico, M.M.; de Lanzós, A.L.; Porteiro, C.; Sagarminaga, Y.; Santos, M.; Uriarte, A.; Cunha, E.; et al. Sardine spawning off the European Atlantic coast: Characterization of and spatio-temporal variability in spawning habitat. *Prog. Oceanogr.* **2007**, *74*, 210–227. [CrossRef]
25. Planque, B.; Bellier, E.; Lazure, P. Modelling potential spawning habitat of sardine (*Sardina pilchardus*) and anchovy (*Engraulis encrasicolus*) in the Bay of Biscay. *Fish. Oceanogr.* **2007**, *16*, 16–30. [CrossRef]
26. Somarakis, S.; Palomera, I.; Garcia, A.; Quintanilla, L.; Koutsikopoulos, C.; Uriarte, A.; Motos, L. Daily egg production of anchovy in European waters. *ICES J. Mar. Sci.* **2004**, *61*, 944–958. [CrossRef]
27. Hsieh, C.-H.; Reiss, C.; Watson, W.; Allen, M.J.; Hunter, J.R.; Lea, R.N.; Rosenblatt, R.H.; Smith, P.E.; Sugihara, G. A comparison of long-term trends and variability in populations of larvae of exploited and unexploited fishes in the Southern California region: A community approach. *Prog. Oceanogr.* **2005**, *67*, 160–185. [CrossRef]
28. Hsieh, C.H.; Chen, C.S.; Chiu, T.S.; Lee, K.T.; Shieh, F.J.; Pan, J.Y.; Lee, M.A. Time series analyses reveal transient relationships between abundance of larval anchovy and environmental variables in the coastal waters southwest of Taiwan. *Fish. Oceanogr.* **2009**, *18*, 102–117. [CrossRef]
29. Busby, M.S.; Duffy-Anderson, J.T.; Mier, K.L.; de Forest, L.G. Spatial and temporal patterns in summer ichthyoplankton assemblages on the eastern Bering Sea shelf 1996–2007. *Fish. Oceanogr.* **2014**, *23*, 270–287. [CrossRef]

30. Guan, L.; Dower, J.F.; Mckinnell, S.M.; Pepin, P.; Pakhomov, E.A.; Hunt, B.P.V. A comparison of spring larval fish assemblages in the Strait of Georgia (British Columbia, Canada) between the early 1980s and late 2000s. *Prog. Oceanogr.* **2015**, *138*, 45–57. [CrossRef]
31. Jan, S.; Wang, J.; Chern, C.S.; Chao, S.Y. Seasonal variation of the circulation in the Taiwan Strait. *J. Mar. Syst.* **2002**, *35*, 249–268. [CrossRef]
32. Jan, S.; Sheu, D.D.; Kuo, H.M. Water mass and throughflow transport variability in the Taiwan Strait. *J. Geophys. Res.* **2006**, *111*, C12012. [CrossRef]
33. Hsieh, H.Y.; Lo, W.T.; Chen, H.H.; Meng, P.J. Larval Fish Assemblages and Hydrographic Characteristics in the Coastal Waters of Southwestern Taiwan during Non- and Post-typhoon Summers. *Zool. Stud.* **2016**, *55*, 18.
34. Hsieh, H.Y.; Meng, P.J.; Chang, Y.C.; Lo, W.T. Temporal and spatial occurrence of mesopelagic fish larvae during epipelagic drift associated with hydrographic features in the Gaoping coastal waters off southwestern Taiwan. *Mar. Coast. Fish.* **2017**, *9*, 244–259. [CrossRef]
35. Lee, M.A.; Lee, K.T.; Shiah, G.Y. Environmental factors associated with the formation of larval anchovy fishing ground in coastal waters of southwestern Taiwan. *Mar. Biol.* **1995**, *121*, 621–625. [CrossRef]
36. Tsai, C.F.; Chen, P.Y.; Chen, C.P.; Lee, M.A.; Shiah, G.Y.; Lee, K.T. Fluctuation in abundance of larval anchovy and environmental conditions in coastal waters off southwestern Taiwan as associated with the El Niño-Southern Oscillation. *Fish. Oceanogr.* **1997**, *6*, 238–249. [CrossRef]
37. Sassa, C.; Konishi, Y. Late winter larval fish assemblage in the southern East China Sea, with emphasis on spatial relations between mesopelagic and commercial pelagic fish larvae. *Cont. Shelf Res.* **2015**, *108*, 97–111. [CrossRef]
38. Sassa, C.; Takahashi, M. Comparative larval growth and mortality of mesopelagic fishes and their predatory impact on zooplankton in the Kuroshio region. *Deep Sea Res. Part I Oceanogr. Res. Pap.* **2018**, *131*, 121–132. [CrossRef]
39. Leis, J.M.; Rennis, D.S. *The Larvae of Indo-Pacific Coral Reef Fishes*; New South Wales University Press: Sidney, Australia, 1983.
40. Ozawa, T. *Studies on the Oceanic Ichthyoplankton in the Western North Pacific*; Kyushu University Press: Fukuoka, Japan, 1986.
41. Okiyama, M. (Ed.) *An Atlas of the Early Stage Fishes in Japan*; Tokai University Press: Tokyo, Japan, 1988. (In Japanese)
42. Leis, J.M.; Trnski, T. *The Larvae of Indo-Pacific Shorefishes*; New South Wales University Press: Sidney, Australia, 1989.
43. Neira, F.J.; Miskiewicz, A.G.; Trnski, T. *Larvae of Temperate Australian Fishes*; University of Western Australia Press: Perth, Australia, 1998.
44. Omori, M.; Ikeda, T. *Methods in Marine Zooplankton Ecology*; Wiley: New York, NY, USA, 1984.
45. Shannon, C.E.; Weaver, W. *The Mathematical Theory of Communication*; University of Illinois Press: Urbana, IL, USA, 1949.
46. Dunn, O.J.; Clark, V.A. *Applied Statistics: Analysis of Variance and Regression*; John Wiley: New York, NY, USA, 1974.
47. Bray, J.R.; Curtis, J.T. An ordination of the upland forest communities of southern Wisconsin. *Ecol. Monogr.* **1957**, *27*, 325–349. [CrossRef]
48. Kruskal, J.B.; Wish, M. *Multidimensional Scaling*; Sage University Paper Series on Quantitative Application in the Social Sciences; Sage Publications: Beverly Hills, CA, USA, 1978.
49. Hosie, G.W.; Cochran, T.G. Mesoscale distribution patterns of macrozooplankton communities in Prydz bay, Antarctica—January to February 1991. *Mar. Ecol. Prog. Ser.* **1994**, *106*, 21–39. [CrossRef]
50. Somarakis, S.; Drakopoulos, P.; Filippou, V. Distribution and abundance of larval fishes in the northern Aegean Sea—Eastern Mediterranean—In relation to early summer oceanographic conditions. *J. Plankton Res.* **2002**, *24*, 339–357. [CrossRef]
51. Anderson, M.J. A new method for non-parametric multivariate analysis of variance. *Aust. Ecol.* **2001**, *26*, 32–46.
52. Mantua, N.J.; Hare, S.R.; Zhang, Y.; Wallace, J.M.; Francis, R.C. A Pacific interdecadal climate oscillation with impacts on salmon production. *Bull. Am. Meteorol. Soc.* **1997**, *78*, 1069–1079. [CrossRef]
53. Wolter, K.; Timlin, M.S. Measuring the strength of ENSO events: How does 1997/98 rank? *Weather* **1998**, *53*, 315–324. [CrossRef]
54. McArdle, B.H.; Anderson, M.J. Fitting multivariate models to community data: A common on distance-based redundancy analysis. *Ecology* **2001**, *82*, 290–297. [CrossRef]
55. Chen, J.M.; Wang, F.J.; Lu, F.C.; Kuo, S.L. El Nifño and 1998 Climate Variability of Taiwan: Persistent Warming and Excessive Spring Rains. *Atmos. Sci.* **2002**, *30*, 331–349.
56. Wang, B.; Wu, R.G.; Fu, X.H. Pacific-East Asian teleconnection: How does ENSO affect East Asian climate? *J. Clim.* **2000**, *13*, 1517–1536. [CrossRef]
57. Kuo, N.J.; Ho, C.R. ENSO effect on the sea surface wind and sea surface temperature in the Taiwan Strait. *Geophys. Res. Lett.* **2004**, *31*, L13309. [CrossRef]
58. Schwing, F.B.; Murphree, T.; Green, P.M. The Northern Oscillation Index (NOI): A new climate index for the northeast Pacific. *Prog. Oceanogr.* **2002**, *53*, 115–119. [CrossRef]
59. Lee, M.A.; Kuo, Y.C.; Chan, J.W.; Chen, Y.K.; Teng, S.Y. Long-term (1982–2012) summertime sea surface temperature variability in the Taiwan Strait. *Terr. Atmos. Ocean. Sci.* **2015**, *26*, 183–192. [CrossRef]
60. Pan, J.; Yan, X.H.; Zheng, Q.; Liu, W.T.; Klemas, V.V. Interpretation of scatterometer ocean surface wind vector EOFs over the Northwestern Pacific. *Remote Sens. Environ.* **2002**, *84*, 53–68. [CrossRef]
61. García-Comas, C.; Stemmann, L.; Ibanez, F.; Berline, L.; Mazzocchi, M.G.; Gasparini, S.; Picheral, M.; Gorsky, G. Zooplankton long-term changes in the NW Mediterranean Sea: Decadal periodicity forced by winter hydrographic conditions related to large-scale atmospheric changes? *J. Mar. Syst.* **2011**, *87*, 216–226. [CrossRef]

62. Feng, J.; Stige, L.C.; Durant, J.M.; Hessen, D.O.; Zhu, L.; Hjermann, D.O.; Llope, M.; Stenseth, N.C. Large-scale season-dependent effects of temperature and zooplankton on phytoplankton in the North Atlantic. *Mar. Ecol. Prog. Ser.* **2014**, *502*, 25–37. [CrossRef]
63. Lo, W.T.; Yu, S.F.; Hsieh, H.Y. Hydrographic processes driven by seasonal monsoon system affect siphonophore assemblages in tropical-subtropical waters (western North Pacific Ocean). *PLoS ONE* **2014**, *9*, e100085. [CrossRef]
64. Marques, S.C.; Primo, A.L.; Martinho, F.; Azeiteiro, U.M.; Pardal, M.Â. Shifts in estuarine zooplankton variability following extreme climate events: A comparison between drought and regular years. *Mar. Ecol. Prog. Ser.* **2014**, *499*, 65–76. [CrossRef]
65. Tseng, H.-C.; You, W.-L.; Huang, W.; Chung, C.-C.; Tsai, A.-Y.; Chen, T.-Y.; Lan, K.-W.; Gong, G.-C. Seasonal Variations of Marine Environment and Primary Production in the Taiwan Strait. *Front. Mar. Sci.* **2020**, *7*, 38. [CrossRef]
66. Auth, T.D.; Brodeur, R.D.; Soulen, H.L.; Ciannelli, L.; Peterson, W.T. The response of fish larvae to decadal changes in environmental forcing factors off the Oregon coast. *Fish. Oceanogr.* **2011**, *20*, 314–328. [CrossRef]
67. Raya, V.; Sabatés, A. Diversity and distribution of early life stages of carangid fishes in the northwestern Mediterranean: Responses to environmental drivers. *Fish. Oceanogr.* **2015**, *24*, 118–134. [CrossRef]
68. Ottersen, G.; Stenseth, N.C. Atlantic climate governs oceanographic and ecological variability in the Barents Sea. *Limnol. Oceanogr.* **2001**, *46*, 1774–1780. [CrossRef]
69. Colton, J.B., Jr. A field observation of mortality of marine fish larvae due to warming. *Limnol. Oceanogr.* **1959**, *4*, 219–222. [CrossRef]
70. McGowen, G.E. Coastal ichthyoplankton assemblages, with emphasis on the southern California bight. *Bull. Mar. Sci.* **1993**, *53*, 692–722.
71. Sanvicente-Añorve, L.; Flores-Coto, C.; Chiappa-Carrara, X. Temporal and spatial scales of ichthyoplankton distribution in the southern Gulf of Mexico. *Estuar. Coast. Shelf Sci.* **2000**, *51*, 463–475. [CrossRef]
72. Rodriguez, J.M.; Hernandez-Leon, S.; Barton, E.D. Vertical distribution of fish larvae in the Canaries-African coastal transition zone in summer. *Mar. Biol.* **2006**, *149*, 885–897. [CrossRef]
73. Watanabe, H.; Sassa, C.; Ishida, M. Late winter vertical distribution of mesopelagic fish larvae in the Kuroshio Current region of the western North Pacific. *Bull. Jpn. Soc. Fish. Oceanogr.* **2010**, *74*, 153–158.
74. Beaugrand, G.; Brander, C.M.; Lindley, A.J.; Souissi, S.; Reid, P.C. Plankton effect on cod recruitment in the North Sea. *Nature* **2003**, *426*, 661–664. [CrossRef]
75. Frank, K.T.; Petrie, B.; Shackell, N.L.; Choi, J.S. Reconciling differences in trophic control in mid-latitude marine ecosystems. *Ecol. Lett.* **2006**, *9*, 1096–1105. [CrossRef]
76. Perry, R.I.; Schweigert, J. Primary productivity and the carrying capacity for herring in NE Pacific marine ecosystems. *Prog. Oceanogr.* **2008**, *77*, 241–251. [CrossRef]
77. DiLorenzo, E.; Schneider, N.; Cobb, K.M.; Chhak, K.; Franks, P.J.S.; Miller, A.J.; McWilliams, J.C.; Bograd, S.J.; Arango, H.; Curchitser, E.; et al. North Pacific Gyre Oscillation links ocean climate and ecosystem change. *Geophys. Res. Lett.* **2008**, *35*, L08607.
78. Mackas, D.; Galbraith, M.; Faust, D.; Masson, D.; Young, K.; Shaw, W.; Romaine, S.; Trudel, M.; Dower, J.; Campbell, R.; et al. Zooplankton time series from the Strait of Georgia: Results from year-round sampling at deep water locations, 1990–2010. *Prog. Oceanogr.* **2013**, *115*, 129–159. [CrossRef]
79. Sassa, C.; Tsukamoto, Y. Distribution and growth of Scomber japonicas and S. australasicus larvae in the southern East China Sea in response to oceanographic conditions. *Mar. Ecol. Prog. Ser.* **2010**, *419*, 185–199. [CrossRef]